Observation of GeV Solar Energetic Particles from the 6 November 1997 Event Using Milagrito

A.Falcone, R.Atkins, W.Benbow, D.Berley, M.L.Chen, D.G.Coyne, B.L.Dingus, D.E.Dorfan, R.W.Ellsworth, L.Fleysher, R.Fleysher, G.Gisler, J.A.Goodman, T.J.Haines, C.M.Hoffman, S.Hugenberger, L.A.Kelley, I.Leonor, J.F.McCullough, J.E.McEnery, R.S.Miller, A.I.Mincer, M.F.Morales, P.Nemethy, J.M.Ryan, B.Shen, A.Shoup, C.Sinnis, A.J.Smith, G.W.Sullivan, T.Tumer, K.Wang, M.O.Wascko, S.Westerhoff, D.A.Williams, T.Yang, G.B.Yodh
(The Milagro Collaboration)

ABSTRACT

Milagrito was an extensive air shower observatory that operated as a prototype for the larger Milagro instrument. Milagrito operated from February 1997 to May 1998. Although it was originally designed as a very high energy (few hundred GeV threshold) water-Cherenkov gamma-ray observatory, it can also be used to study solar energetic particles (SEPs). By recording scaler data, which corresponded to PMT singles rates, it was sensitive to muons and small showers from hadronic primary particles above ~4 GV. Milagrito simultaneously recorded air shower triggers, which required primary particles with particularly high energies and provided the data necessary to reconstruct event directions. The scalers of Milagrito registered a ground level enhancement associated with the 6 November 1997 SEP event and X9 solar flare. At its peak, the enhancement was 22 times the background RMS fluctuations. Based on comparisons to neutron monitor and satellite data, we find evidence that the rigidity-power-law spectrum for the differential flux of energetic protons at low energies became steeper above ~4 GV, and that the acceleration site was in the low corona (~2 solar radii above the photosphere) if a CME-driven shock mechanism is assumed.

1. Introduction

Particle acceleration to energies greater than 1 GeV due to solar processes is well established (e.g. Meyer et al. 1956, Parker 1957). However, few data exist demonstrating acceleration of particles above 5 GeV (Chiba et al. 1992, Lovell et al. 1998). The energy upper limit of solar particle acceleration is unknown, but it is important because it relates not only to the nature of the acceleration process, itself not ascertained, but also to the environment at or near the Sun where the acceleration takes place. Due to their small size, space-based instruments are relatively ineffective at measuring the low fluxes of particles above ~1 GeV. However, neutron monitors become efficient at these energies. Neutron monitors provide an integral measurement of the particle intensity above a threshold determined by the location of the monitor within the geomagnetic field (Debrunner 1994, Simpson 1957). As energy increases, the SEP spectra typically fall faster than the effective areas rise for neutron monitors. Using the global network of neutron monitors, one can often extract energy information from the different count rates at neutron monitor stations at different geomagnetic cutoffs. This implies that no energy information exists in the neutron monitor data above ~14 GV, which corresponds to the cutoff of an equatorial station. In the past, underground muon telescopes have been used to study the higher energy SEPs, but their effective areas are small and their energy

threshold is far above that of neutron monitors. Other instruments are necessary to study the SEP intensity at higher energies.

Milagro and Milagrito are capable of studying these high energy SEP events by operating at high energies with large areas. The energy threshold of Milagrito was lower than the thresholds of underground muon telescopes and traditional extensive air shower arrays, while the effective area of Milagrito was much larger than that of neutron monitors. For the showers that were incident on the detectors sensitive area, Milagrito could detect a relatively large fraction of the secondary particles from air showers by utilizing the water Cherenkov technique in a large, water-filled pond. This increased sampling of shower particles relative to that of traditional extensive air shower arrays, which are insensitive below the TeV regime, contributes to the lower energy threshold of Milagro and Milagrito. This technique also leads to an effective area that is more than three orders of magnitude greater than that of neutron monitors above ~4 GV. With an intrinsic rigidity threshold for vertical protons of ~3.9 GV, due to the location of the detector within the Earth's geomagnetic field, Milagro/ito measurements complement those of the neutron monitor network. An increased sensitivity to high-energy, anisotropic events can also be achieved when Milagro/ito is able to reconstruct incident directions of the primary particles.

Coronal mass ejections (CMEs) and solar flares are frequently accompanied by SEPs, but the details of the acceleration process(es) continue to elude researchers. Although SEP events are frequently categorized as either gradual or impulsive (Reames 1999, Gosling 1993), some events do not seem to fit neatly into either category (Mobius et al. 1999). Gradual events generally exhibit greater fluxes of SEPs over long time scales and tend to be associated with long-duration type II/IV radio emission, coronal-like ion abundances, and low electron-to-proton ratios. On the other hand, impulsive events typically exhibit smaller fluxes of SEPs over shorter time scales. They also tend to be associated with large electron-to-proton ratios and enhancements in heavy ions and ^{3}He. Fast (velocity greater than 400 km/s) CME-driven coronal and interplanetary shocks are generally thought to be the acceleration mechanism for the gradual events (Lee 1997, Kahler 1992), while the impulsive events are frequently thought to originate at the flare sites (Reames 1999).

On 6 November 1997 at 11:49 UT, an X9 flare with an associated coronal mass ejection (CME) occurred on the western hemisphere of the Sun. This event was well observed with many instruments, and it exhibited both gradual and impulsive characteristics. The GOES-9 satellite detected energetic protons in excess of 100 MeV, and hard X-rays were detected by GOES-9 and the Yohkoh HXT (GOES 2001, Sato et al. 2000). Yohkoh also recorded impulsive gamma-ray emission up to 100 MeV for approximately 5 minutes, along with the presence of gamma-ray lines (Yoshimori et al. 2000). LASCO detected the launch of the CME from the Sun, and the speed of the leading edge was estimated to be between ~1600 km/s and ~2200 km/s (St. Cyr 2001, Cliver et al. 2001). Metric radio emission was also observed during this event (Maia et al. 1999). Using ACE measurements, Cohen et al. (1999) and Mason et al. (1999) reported exceptionally hard ion spectra above 10 MeV/nucleon. Furthermore, Fe and ^{3}He enhancements (^{3}He/^{4}He~4times coronal and Fe/O~1) were evident in the interplanetary particle populations at these energies energies. These values are greater than those expected for a gradual event, but the enhancements are not as great as those found in many impulsive events.

There were also ground-based measurements of this event. Many of the instruments in the world-wide network of neutron monitors registered a ground level enhancement (GLE) in response to protons with energies in excess of ~1 GeV (Duldig et al. 1999). The rate increase began shortly after 12:00 UT with an anisotropic component,

but the distribution approached isotropy by the time of maximum, approximately 45 minutes after the onset (Lovell et al. 1999). Low latitude monitors, such as Mexico City (cutoff rigidity ~ 8.6 GV) did not record an increase. The Climax neutron monitor, located less than 400 km north of the Milagrito site with a vertical cutoff rigidity of ~3 GV, was among those to record a rate increase.

2. Milagrito Instrument Description

Milagrito was located near Los Alamos, NM at an elevation of 2650 m (750 g/cm^2 atmospheric overburden). It operated as a prototype for the Milagro instrument from February 1997 to May 1998 (Atkins et al. 2000; McCullough et al. 1999). The detector was composed of 228 upward-facing photomultiplier tubes (PMTs) submersed in 1 to 2 meters of "clean" water (attenuation length of about 5 m for light at a wavelength of 350 nm). These tubes were placed within an 80×60×8 m pond, under a light-tight cover, in a square grid pattern with 2.8 m spacing between each PMT. When an energetic hadronic particle or gamma ray is incident on the Earth's atmosphere, it can induce an extensive air shower (EAS) that propagates downward in the form of a thin (~1-3 m) "pancake-like" plane of secondary particles. Upon entering the water of the Milagrito pond, the charged particles from the EAS produce Cherenkov light that is emitted in 42˚ cones. These Cherenkov photons are then detected by the PMT array. The gamma rays in the EAS undergo both Compton scattering and pair production when they enter the water, thus contributing to the Cherenkov photons detected in the pond. With this technique, a large fraction of the shower particles that strike the pond can be detected, and a low threshold energy is achievable.

Designed as a very high energy (VHE) gamma ray observatory, Milagrito's air shower trigger was sensitive to extensive air showers from primary hadrons and gamma rays above ~100 GeV. Milagrito required 100 PMTs to record a signal in coincidence in order for the data acquisition hardware to record an air shower trigger event. For a PMT to contribute to this trigger its pulse height had to exceed a threshold corresponding to ~0.25 photoelectrons, referred to as the low threshold. For each event, the time and pulse height in each PMT were recorded. The time-over-threshold technique was used to measure pulse height. Once these data were recorded, they could be used to reconstruct the incident direction of the primary particle with a resolution of less than 1˚. The hadron-induced showers were treated as background for the studies of gamma ray sources using the air shower trigger data, but hadron-induced events were treated as a signal for the purposes of solar and cosmic ray physics.

In addition to recording these air shower trigger events, thus operating as a telescope, Milagrito also recorded scaler data that corresponded to PMT singles rates. These data are similar to that of a neutron monitor. The value that is recorded is a time-integrated measurement that corresponds to the rate of single PMT hits in the pond. For the purposes of this scaler counting, a PMT was considered to be hit when its pulse height exceeded a threshold corresponding to ~7.6 photoelectrons, referred to as the high threshold. This high threshold output has considerably less background fluctuation (due to its reduced sensitivity to small quantities of light that may come from instrumental sources or other systematic effects) than the low threshold output used for the air shower trigger. This is important when considering the large number of smaller and unreconstructable events registered by the scalers. The PMTs were separated into 15 4×4 patches, and the scalers counted the number of patches that registered at least one hit during a ~45 ns interval. The number of scaler hits was read with a period of 1 second.

Since the energy range most likely to be of primary interest to solar physics is <100 GeV, the scaler counting ability of Milagrito is extremely useful, despite the fact

that reconstruction of event directions is not possible with these data. By recording this scaler data, an integral measurement above a hardware-defined threshold is performed. These data provide a high energy complement to the network of neutron monitors.

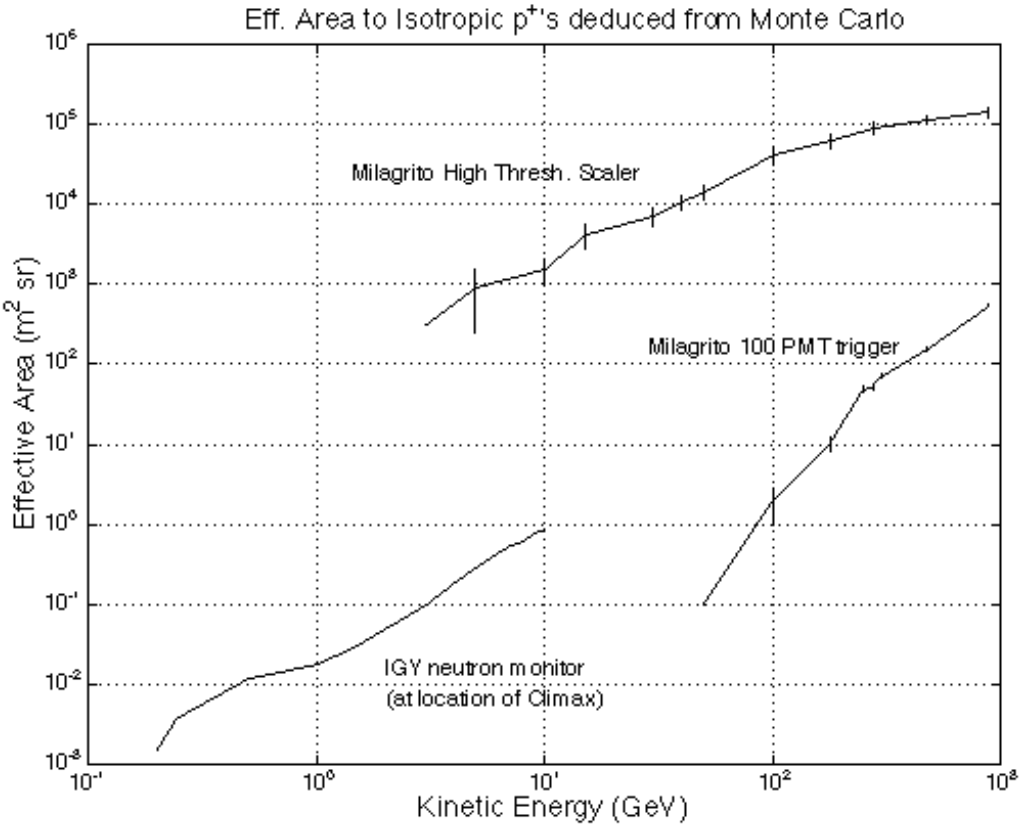

Fig. 1 – Effective area of Milagrito to isotropic protons incident on the top of the Earth's atmosphere, with an IGY neutron monitor for comparison. These calculations are based on Monte Carlo proton events thrown over zenith angles of 0˚-60˚, with extrapolated values used for zenith angles from 60˚-90˚.

With an analysis based on the Monte Carlo calculations, effective areas of the Milagrito instrument were computed. For the purpose of simulating Milagrito's response, effective area is defined as: $(N_{trigger}/N_{throw})A_{throw}$, where A_{throw} is the area over which the shower core is thrown and $N_{trigger}$ and N_{throw} are the number of triggers and the number of primary particles thrown, respectively. Of particular interest for solar ground level events are the effective areas of Milagrito for protons incident on the atmosphere isotropically, at zenith angles ranging from 0º-90º (Figure 1). The curves shown in the figure correspond to the effective areas of the high threshold scalers and the air shower trigger. The effective area from 60º-90º was estimated by extrapolating the area curve from the 0º-60º range, which was simulated with the Monte Carlo. In the absence of effects specific to large zenith angles, the majority of the contribution to the scaler efficiency comes from zenith angles below 60˚. An example of the relative contribution at angles above and below 60˚ for protons at 50 GeV can be seen in figure 2. Since cosmic ray showers were not simulated between 60º-90º due to limitations of the software and time, effects that are present only at large zenith angles are not reflected in these effective area curves (see section 3.2). While this could have a significant impact on the analysis of the air shower data, which may be more prone to unsimulated effects specific to high zenith angles, it should not significantly affect the scaler data.

The complete simulation of the detector response was performed in two steps. The initial interaction of the primary particle with the atmosphere and the generation of secondary particles was simulated with the CORSIKA air shower simulation code (Heck et al. 1998). The primary particles and shower particles are tracked through the atmosphere, which is stratified into five horizontal layers. When the particles initiate a reaction or decay, the secondary particles are also tracked through the atmosphere. Electromagnetic interactions are simulated using EGS 4 code. For the hadronic interactions, the VENUS code is used at high energies, and GHEISHA is used at low energies (<80 GeV). The second step was to simulate the response of the detector itself using GEANT (CERN 1994).

The areas in figure 1 were calculated using Monte Carlo events whose shower cores were thrown randomly over a large area surrounding the Milagrito pond. To ensure that the Monte Carlo showers were thrown over a large enough area, we progressively increased the throw area until the effective area reached an asymptotic value. This occurred at approximately 7000×7000 m^2. Figure 3 illustrates the relationship between Milagrito's calculated effective area and the shower-core throw area for 50 GeV protons. We note that the effective area of Milagrito has a significant contribution from hadronic showers with cores far (> 3 km) from the detector. This effect increased the estimated effective area at ~5-100 GeV by ~3 orders of magnitude relative to earlier estimates, which used a throw dimension of 100 m (Falcone et al. 1999, Ryan et al. 1999).

The systematic errors of the instrument response have been estimated by folding the known cosmic ray spectrum through the calculated response. This results in a

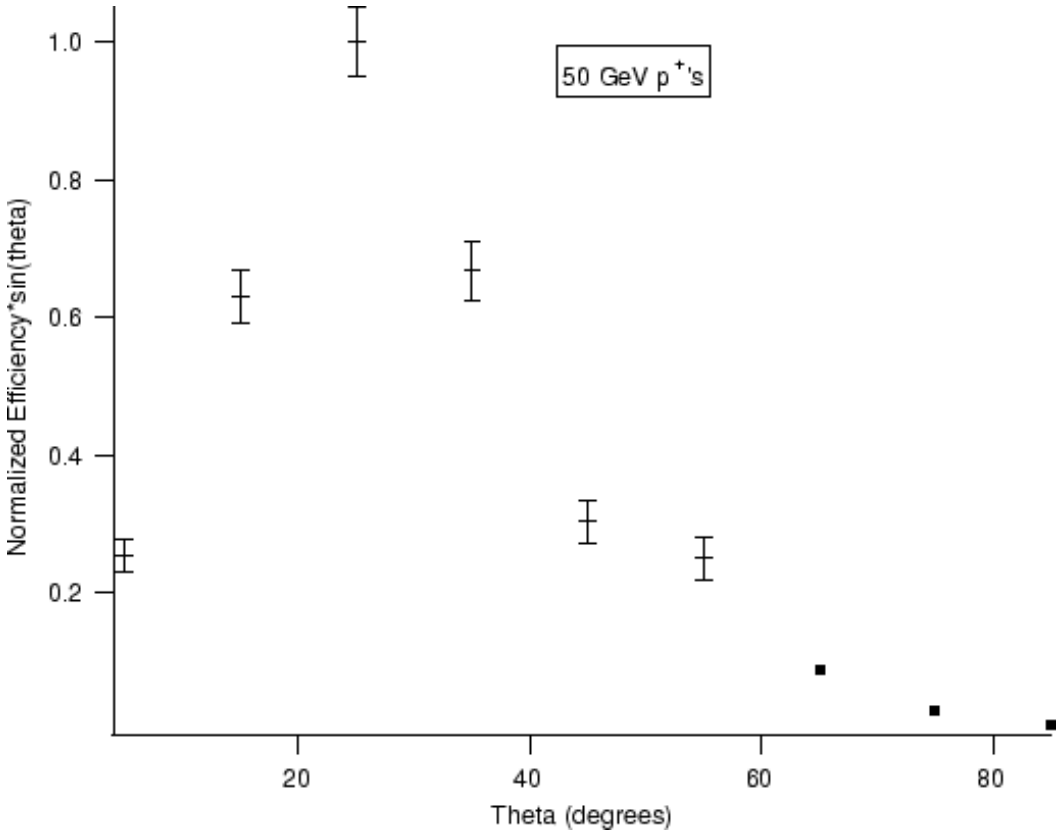

Fig. 2 – Differential efficiency of Milagrito scalers to 50 GeV protons (from Monte Carlo) normalized to 25˚ and plotted as a function of zenith angle. Points above 60˚ are extrapolated using a functional fit (using a polynomial multiplied by sin θ) to smaller values of θ. The contribution from θ>60˚ is shown to be small.

theoretical value for the instrument's rate due to galactic cosmic rays, which comprise most of the instrument's background rate. Although the simulation predicts a rate that is higher than the observed rate, the measured background scaler rate in Milagrito matches this predicted value to within a factor of ~3. While this provides us with a level of confidence in the calculated effective area curves, there are still some concerns. There are some concerns with using GHEISHA to simulate showers from primary particles with energies below ~20 GeV (Heck 1999). For these lower energy primary particles, it is possible that the sum of the secondary shower particle energies can be as much as 20-

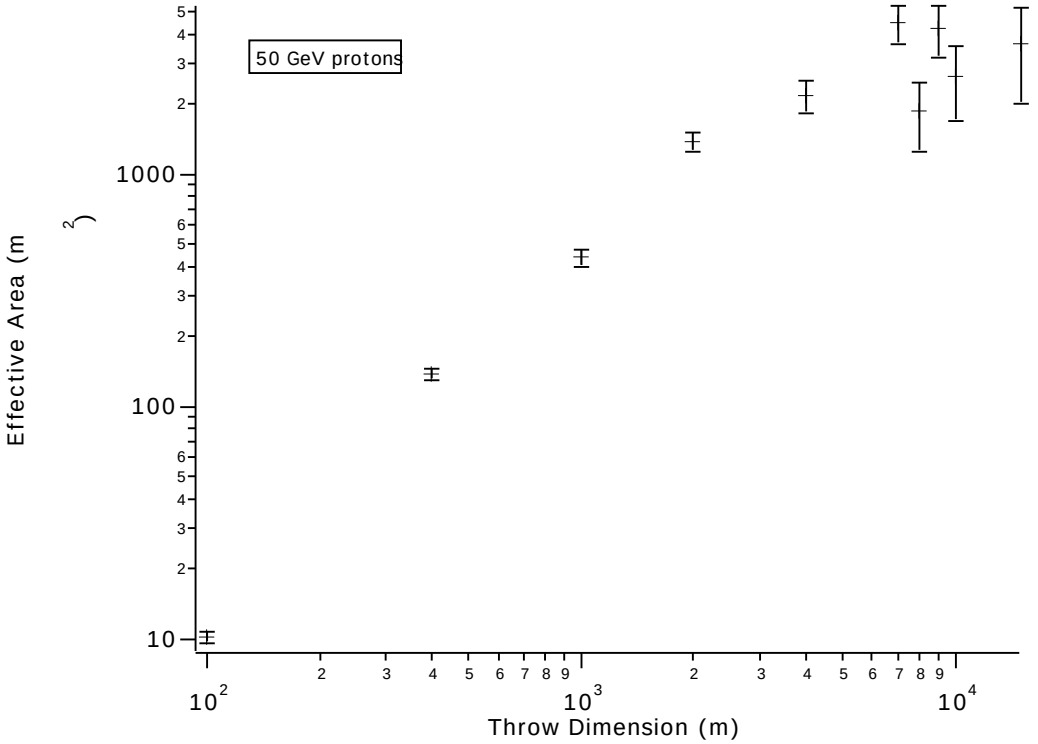

Fig. 3 – An example of the relationship between effective area of the Milagrito scalers and the spatial dimensions over which the simulation throws the shower cores. The area increases with the square of the throw dimension for relatively small throw dimensions. An asymptotic value is approached when the throw dimension becomes large enough to overcome the transverse momentum of the EAS. The size of the error bars increases at large throw dimensions due to the small number of simulated events that result in a signal at the Milagrito pond.

30% greater than the energy of the primary hadron. While a reasonable agreement (factor of ~3) between the predicted and the measured cosmic ray rates in the Milagrito scalers shows that the effective area systematic errors are reasonably small, we are unable to assess the effect of using GHEISHA at energies below ~20 GeV.

At 10 GeV, the high-threshold scaler effective area of Milagrito was ~3 orders of magnitude greater than that of a sea level neutron monitor, with the effective area rising rapidly with energy. The threshold of Milagrito is defined by the combined effects of the geomagnetic field and atmospheric attenuation. The effects of the atmosphere, for zenith angles between 0˚-60˚ degrees are incorporated into the effective area curves, while higher angles are assumed to be a simple extrapolation of the curve, as depicted in figure 2. The geomagnetic effect is incorporated by assuming a hard cutoff at the calculated vertical cutoff rigidity, which is ~3.9 GV. The fact that this is actually a function of

zenith angle and magnetic field fluctuations should be considered when interpreting the response of the detector.

To analyze the scaler data of Milagrito properly, one must first correct the ground level scaler rates for atmospheric pressure, temperature, and other diurnal effects (Hayakawa 1969). Typical background cosmic ray rate fluctuations on a time scale of ~1 day are shown in figure 4. Although this figure shows the pressure at ground level, which is not as critical as the measurement of pressure at higher altitudes in the atmosphere, one can clearly observe the increase in background rate as the pressure, and consequently the atmospheric overburden, decreases. Atmospheric temperature also effects the background rate, as a result of the variation of muon lifetime with temperature. Although this smaller effect can not be seen in the figure due to the overwhelming pressure variation, which can be on the order of -5 to -10 %/inHg, the overall temperature

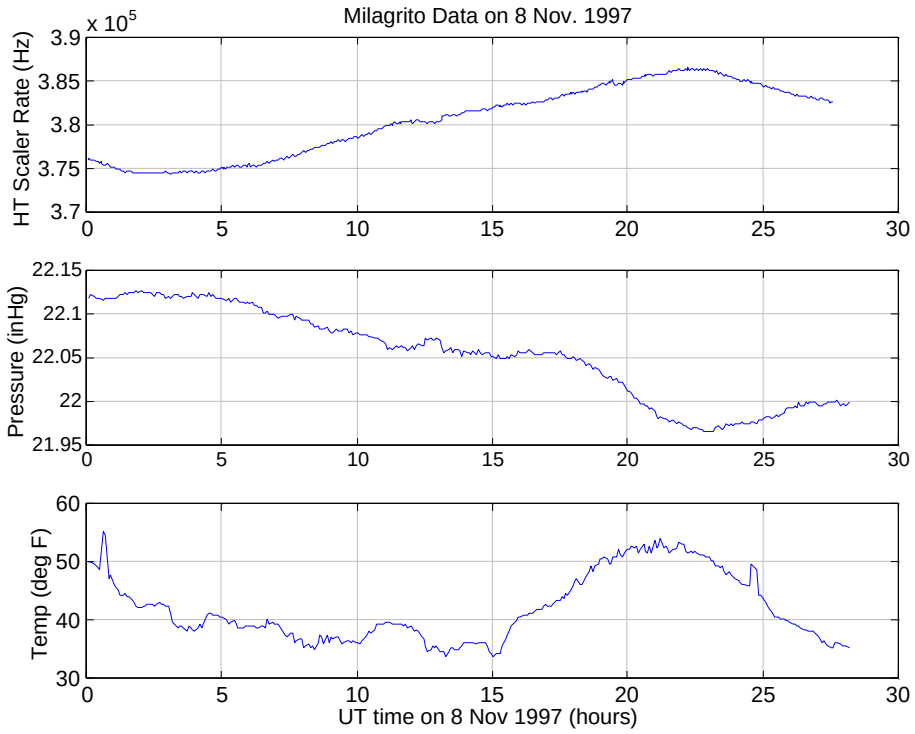

Fig. 4 – Typical diurnal fluctuations in Milagrito scaler rate during a time period which is relatively free of instrumental anomalies.

effect can cause variations on the order of -5×10^{-2} %/˚F. Preliminary estimates of these correction factors for Milagro/Milagrito have been calculated based on observations, and they have been found to be reasonably consistent with past work with muon telescopes (Fowler et al. 1961). Accurate estimates of the pressure and temperature correction factors for Milagrito have not been calculated due primarily to the multitude of variations on many timescales that were present in the Milagrito data. This was a result of the fact that Milagrito was an engineering prototype that had significant variation in detector parameters such as water level, electronic thresholds, and light-leak integrity of the cover. However, these atmospheric corrections are less important for fast transient events that rise above background quickly and have short durations.

3. Observations of 6 November 1997 Event Using Milagrito

Since their sensitivities are different, the scalers and the air shower triggers are analyzed separately.

3.1. *Scaler Observations*

Milagrito measured a scaler rate increase coincident, within error, with the increase observed by Climax (see figure 5). If one accounts for the background meteorological fluctuations that are present, the event duration and time of maximum intensity, as seen with Milagrito, are also consistent with that of Climax. The magnitude of the scaler rate increase is ~22 times the RMS fluctuations of the instrument's background using 160 second time bins. The background scaler rate prior to the event was ~375 kHz, and the event produced a rate increase of ~0.5 % from the onset to the time-of-maximum. The RMS of observed background fluctuations during a two hour period prior to the event onset, which is approximately ± 84 Hz, is nearly twice that expected from Poisson statistics. These larger fluctuations may be a result of effects such as meteorological fluctuations in the upper atmosphere and at the Milagro site. We also estimated the chance probability of an event rate increase of this magnitude, over this time scale, by looking at the data over the lifetime of Milagrito. This was done by splitting all of the Milagrito high threshold scaler data into 10 minute time bins. The difference between the average rate in any two time bins separated by one hour from the start of one bin to the start of the next was then calculated. There were only two other rate increases of at least this magnitude during the 15 month (no data recorded for ~20%

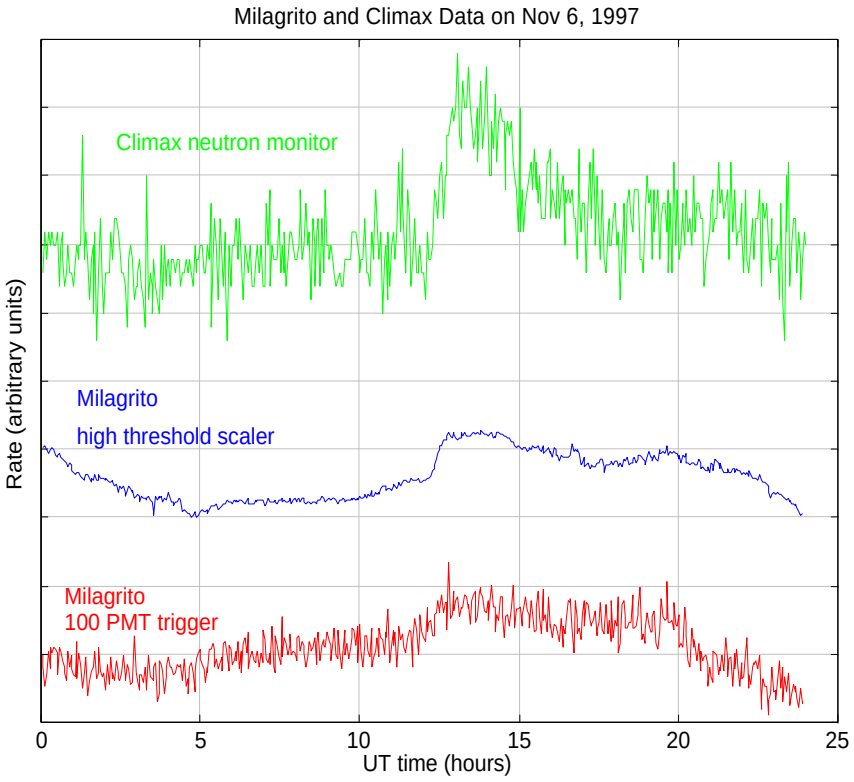

Fig. 5 – Milagrito high-threshold scaler rate and air shower trigger rate plotted over the same timescale as the nearby Climax neutron monitor. The high threshold scaler rate increase of Milagrito was coincident with the rate increase observed by Climax. Diurnal background variations are also visible in the Milagrito data.

of this time due to maintenance, hardware reconfigurations, etc.) lifetime of the instrument. One of these is a possible light leak, and the other has been identified as a power up transient effect. We have found that the probability for a chance rate increase with a magnitude and timescale similar to that of the 6 Nov.1997 event is $\sim 2\times10^{-4}$, or less. This number represents the upper limit to the probability of detecting this event if a blind search was carried out over the entire lifetime of Milagrito (including all of its systematics), whereas the 22 times RMS rate increase was actually well correlated in time with other observations on 6 November 1997.

We note that the scaler rate plotted in figure 5 does not include one of the 15 patches of the detector. This historically noisy group of PMTs, located within patch 7, exhibited an unrelated instrumental rate increase a few hours after the onset of the CME related rate increase. This type of instrumental rate increase (referred to as "flashing" and thought to be caused by arcing in the base or light emission in the tube) is common in some clusters of PMTs, but it can be identified and corrections can be applied based on its localized spatial characteristic. A "flasher" will cause a disproportionate rate increase in a local cluster of PMTs, but an air shower signal will cause a more uniform increase over the entire pond. During the rate increase on 6 November 1997, all of the patches except for patch 7 experienced a uniform rate increase with an average increase of 0.48% and a standard deviation of 0.08%. Patch 7 experienced a rate increase of 1.1% ±0.03%. After studying the uniformity of the signal over the pond in this way and analyzing the instrument's behavior over its lifetime, we concluded that an instrumental increase could be attributed to patch 7. The other patches exhibited a uniform increase of solar origin. It is this rate increase, with patch 7 subtracted, that is shown in the figure and used in the present analysis.

3.2. *Air Shower Trigger Observations*

The air shower trigger also experienced a rate increase, although the significance is not as great as that in scaler mode. The magnitude of the air shower trigger rate increase is ~2 times the RMS fluctuations of the background using 160 sec time bins, the same timescale used for the scalers (RMS is calculated using several hours of data immediately prior to the event onset). Relative to the scaler data, the RMS fluctuations of the air shower trigger data are closer to that expected from Poisson statistics, but they are still slightly larger. Another estimate of the significance that considers longer timescales was obtained by finding the RMS fluctuations on larger timescales and on several days in November. By looking at the RMS fluctuations in 1 hour time bins between 10:00 UT and 17:00 UT on 6 days in November, the air shower trigger event rate excess was found to be ~1.3 times the fluctuations. We expected that the shower trigger would have a smaller response to an event such as this because the shower trigger has a higher threshold energy and has a smaller effective area.

While this significance is marginal, the apparent rate increase at the same time as the other observations of the solar event must be evaluated. The motivation for this is to elucidate any potential impact on the scaler analysis, as well as other ground level observations.

The air shower trigger provides data that is nominally more stable than the scaler data. In spite of this, there are some effects that can lead to a misinterpretation of the air shower trigger data, while not causing an effect in the scaler data that will be significant relative to its larger background. If a mechanism for causing an air shower trigger that is not modeled by the effective area curves in figure 1, such as those to be listed in the following paragraphs, is present then it may lead to a small event rate increase. While this increase may appear in the air shower rate, the corresponding rate increase in the

high threshold scalers, which may be between 7 and 15 times as many Hz, will not be significant over the much larger background of the scalers. With this in mind, several potential mechanisms and instrumental effects for causing rate increases in the air shower trigger have been considered. Some of the explanations for the apparent shower trigger rate increase that have been considered are isotropic proton primaries (such as those that caused the high threshold scaler increase, but with much higher energies), instrumental effects, and high zenith angle muons.

The air shower trigger effective area curve in figure 1 represents the response of this triggering scheme of Milagrito to isotropic protons, but the simulated response does not include effects at high (>60˚) zenith angles. It is evident from this curve that particles of much higher energies (on the order of 100 GeV or greater) are needed to induce a

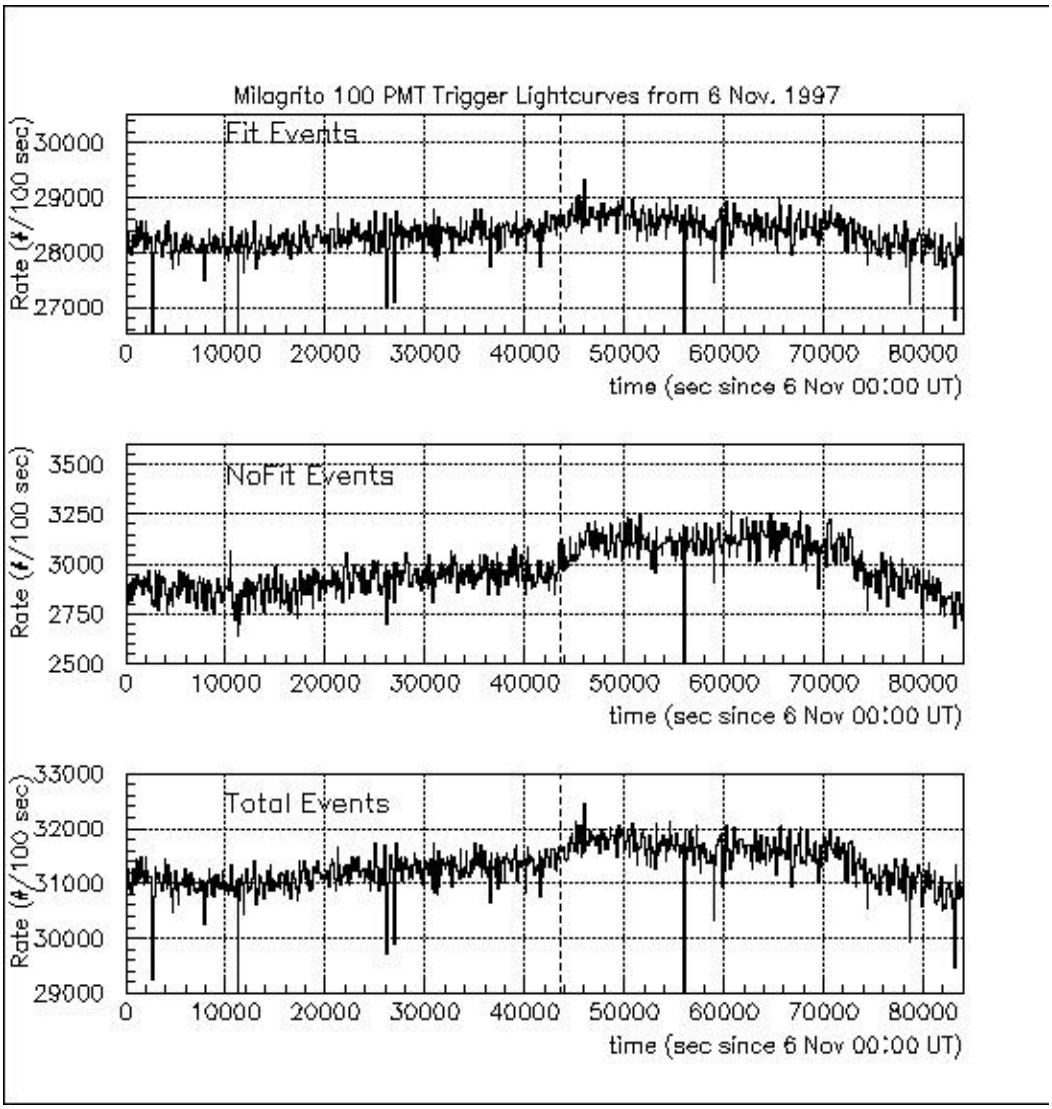

Fig. 6 – Comparison of the air shower trigger time histories for fittable and unfittable events. It is apparent that the ratio of events that cannot be fit to events that can be fit increases during the time of the event. (The dashed line marks the onset of the event according to the high threshold scalers.)

response using this trigger with any reasonable input spectrum, as compared to the particle energies required for a signal in the scalers. Although the small apparent increase in the air shower trigger rate could have been caused by isotropic, very high

energy primaries (>100 GeV) to which the effective area curve in figure 1 corresponds, it is unlikely. Evidence for this can be found by looking at the quality of the fit to the air shower incident angle during the apparent rate increase. Although 100 PMTs must be hit for the air shower trigger, not all of these PMTs are suitable to be used in the angular reconstruction, also known as fitting the event. For example, some PMTs may be hit significantly later or earlier than expected relative to others, thus giving the impression that there is no coherent shower plane. Individual PMTs that contributed disproportionately to the χ^2 of the fit or had a low pulse height were not included in the fitting procedure. The number of PMTs used in the fit is referred to as N_{fit}. For more detail on the fitting procedure, see Atkins et al. (2000). The events that caused the apparent shower trigger increase on 6 Nov. 1997 all had a low N_{fit} (see figure 6), and many events could not be fit at all. If this rate increase was due to an isotropic proton distribution, as that modeled between zenith angles of 0^o-60^o, then greater numbers of fittable PMTs would be expected since these events lead to "pancake-like" shower fronts, which have a characteristic time delay from one PMT to another. We also see (figure 7) that the fraction of events that cannot be fit increases as the apparent rise in trigger rate progresses. Furthermore, if this increase was due to isotropic protons, then a very hard rigidity spectrum ($P^{-2.5}$, with ~90% of the events from >200 GV) is necessary to explain the increase. This spectrum would conflict with the spectrum inferred from the Milagrito high-threshold scaler rate increase (to be discussed in the next section), as well as neutron monitor and satellite data.

This apparent shower trigger rate increase does not appear to conform to known instrumental effects. One potential source for an instrumental rate increase is a temperature variation in the electronics boards. The temperature of the electronics in Milagrito was monitored, and no correlation between variations of board temperature and trigger rate were evident during this event. Another potential source for an instrumental rate increase is "flashing" PMTs. Flashers, which are caused by light emission at the base and/or in the tube of the PMT, are a common problem with water Cherenkov detectors. There are three known forms of flashers in the Milagrito data that could, in theory, contribute to the air shower trigger rate.

One of these forms of flashers is referred to as a "high PE, low N_{fit}" flasher. This type of flasher, which typically does not lead to high scaler rates, is characterized by particularly high photoelectron hits in individual PMTs. These flashers tend to present themselves in the data with a low number of PMTs that are useable in the fitting procedure (i.e. low N_{fit}), and they tend to disappear completely if an N_{fit} cut of 40 PMTs is applied. This type of flasher is not present at anytime during the event.

Another form of flasher is referred to as a "high PE, high N_{fit}" flasher. This phenomenon may actually be a result of mis-calibration of individual PMTs, rather than an actual flashing in the PMT itself. Like the previous form, these flashers typically do not lead to high scaler rates, and they are characterized by particularly high photoelectron hits in individual PMTs. The difference is that these flashers continue to appear in the data with a high value for N_{fit}. This form of flasher is present during the onset of the event, but this flashing is present before and after the event as well. Since the flashing, or possible calibration effect, remains constant prior to and throughout the event, it cannot be responsible for the observed rate increase.

The third form of flasher, known as a high-rate flasher, is the same one that caused the high rate flashing in patch 7 that was discussed in the earlier section on the scaler observations. This type of flasher is not present in the air shower trigger during the onset of the event, although particularly high rate flashing that contributed to the scaler rate did occur several hours later within patch 7.

There is another potential mechanism by which primary protons can lead to an air shower trigger. High zenith-angle protons leading to secondary muons arriving from nearly horizontal directions could trigger the detector. These events were not simulated since they are from primaries beyond 60°. The increase in the rate of unfittable events as the apparent rate increase progresses (figure 7) is evidence for high zenith-angle muons being the cause of the apparent trigger rate increase. We determined that the majority of unfittable events in the background rate could be attributed to muons from zenith angles > 83°. Thus, it is known that this mechanism can cause an air shower trigger. The

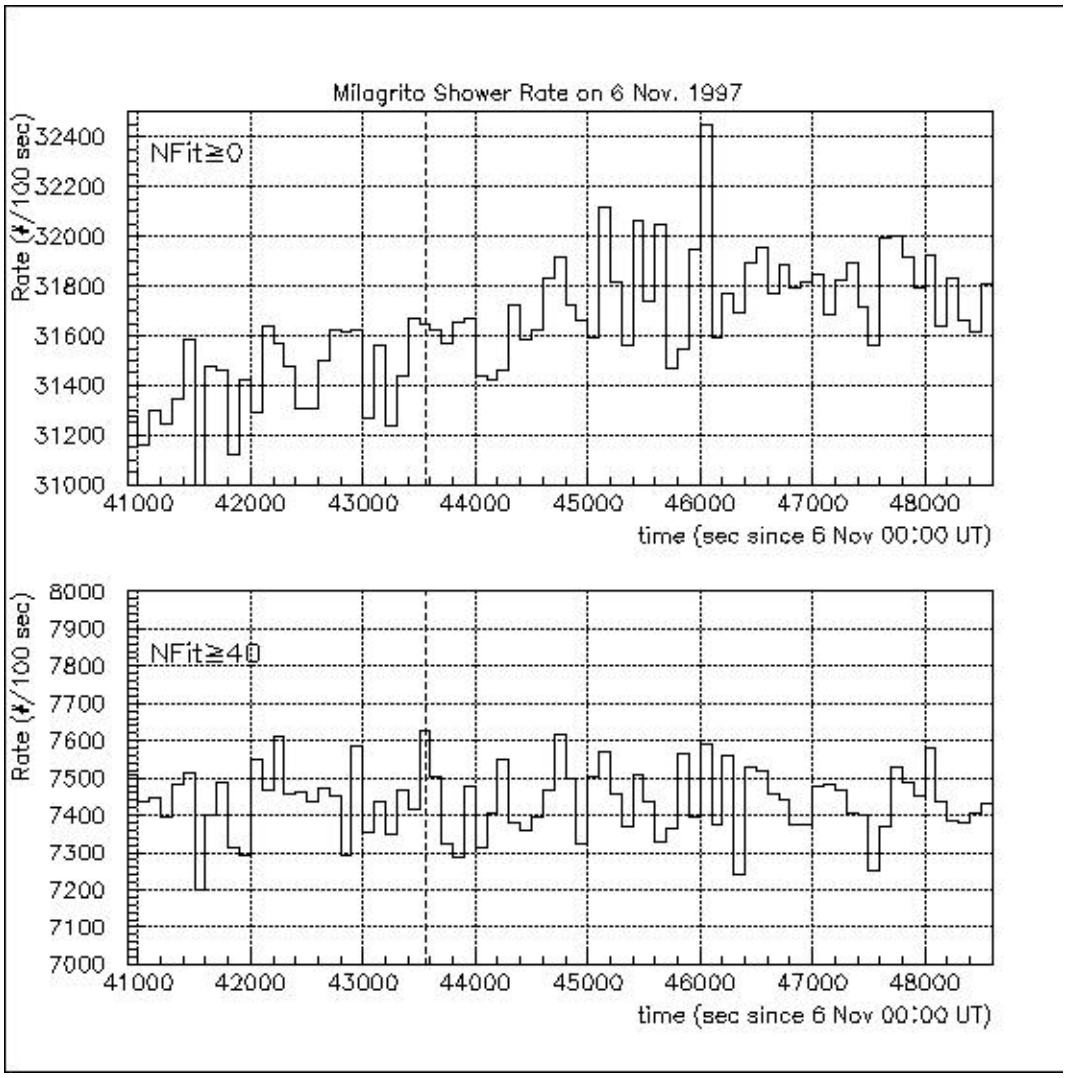

Fig. 7 – Milagrito air shower trigger rate history at the time of the GLE. The top panel includes all events. The bottom panel, which displays no rate increase, includes only the events for which >39 tubes were suitable for use by the angle fitter. The dashed line is the event onset time according to the high threshold scalers.

efficiency of this mechanism for converting a high-zenith-angle proton into a high-zenith-angle muon, and subsequently triggering the detector, is not known. If horizontal muons contributed to this apparent rate increase, they would have been the result of high energy proton primaries (>30 GeV), based on estimates of muon losses in the atmosphere. The effective area curve in figure 1 would not apply to this triggering mechanism. In order to determine the spectrum of the primary protons associated with this mechanism, extensive and time-consuming simulations will have to be completed.

Until more studies and simulations beyond 60˚ are performed, the details of the apparent shower trigger rate increase will not be known. Presently, the work on this apparent increase remains inconclusive. Therefore, this analysis is restricted to the scaler rate increase, based on the belief that if the apparent air shower trigger rate increase is of solar origin, it arises from a response characteristic of the instrument that has not been studied thoroughly. Investigation of the instrument response to primary particles beyond 60˚ is planned.

4. Proton Spectrum based on Milagrito and Neutron Monitor Data

Using only the high-threshold scaler rate increase of Milagrito, we can derive characteristics of the primary proton spectrum. We did this by folding a trial power law spectrum of protons through the response of the instrument. The trial power law spectrum is of the form:

$$f = C(P/P_o)^{-\alpha} ,$$

where P is rigidity [GV] and f is the differential proton flux [m^{-2} s^{-1} sr^{-1} GV^{-1}]. The expected rate increase in the detector, for a given C and α, is then found by integrating:

$$R = \int_{P_{cutoff}}^{\infty} f(P) A_{eff}(P) dP$$

The parameters of the trial spectra, C and α, are then varied until a good fit to the measured rate increase is achieved. By only using the high-threshold scaler rate in this analysis, a range of acceptable values for C and α was determined. To uniquely determine the parameters, another detector with a different response is necessary.

We made the assumption that the geomagnetic rigidity cutoff can be accurately represented by a single value, namely the vertical cutoff rigidity of ~3.9 GV. This ignores any fluctuations in the planetary magnetic field, as well as the change in the cutoff at other zenith angles. Additionally, the pitch angle distribution of protons from the event is assumed to be isotropic. This is a reasonable assumption since it has been shown by other researchers (Lovell et al. 1999, Smart & Shea 1998) that the distribution was approaching isotropy by the time of maximum intensity, which is the time that is being analyzed here. During the onset of the event, at ~12:30 UT, the full-width-half-maximum (FWHM) of the pitch angle distribution was measured by Lovell et al. to be ~60˚, and by ~13:30, at which time the rate increase was on a plateau at maximum, the pitch angle distribution FWHM was ~105˚.

After obtaining the range of spectral parameters from the Milagrito data, we compared this to the spectrum obtained by the worldwide network of neutron monitors. Neutron monitor data for this proton event, near the time of maximum intensity (~12:45-13:00 UT), indicate a rigidity power-law spectral index between approximately 5.2 and 6 in the 1-4 GV rigidity range (Duldig et al. 1999, Lovell et al. 1999). If the Milagrito derived range of spectral parameters for protons above 4 GV is constrained to match the neutron monitor flux at 4 GV and if an unbound power law above 4 GV is assumed, then a unique solution for the spectrum above 4 GV can be obtained. Doing this, we found that the spectral index, α, that best fits the data is 9.0 ± 2.3. (The error bars for the spectral parameters are obtained by doing the above integral with the input parameters modified by their 1σ error bars. The error is dominated by the error in the calculated effective area. Statistical errors from background fluctuations and errors arising from the fitting technique are also included, but the contribution from these error sources is insignificant compared to the effective area error.) The analysis leading to this spectral

index assumes a single power law above 4 GV. We also performed the analysis with a hard upper rigidity cutoff in the proton spectrum, rather than the spectral break described above. We varied this cutoff rigidity as a free parameter while extending the spectrum derived from the neutron monitors up into the energy range of Milagrito. In order for the Milagrito scaler data and the neutron monitor data to be consistent, the hard cutoff must occur at 4.7 ± 0.5 GV (error source as described above), if we assume that the $P^{-5.2}$ spectrum of Lovell et al. (1999) extends into the energy range of Milagrito.

Both of the cases described above are shown in figure 8. These results provide evidence for a cutoff or a rollover in the spectrum in the transition region between the neutron monitors and Milagrito. This is most likely of the form of a progressive spectral softening throughout the energy region above ~1 GeV.

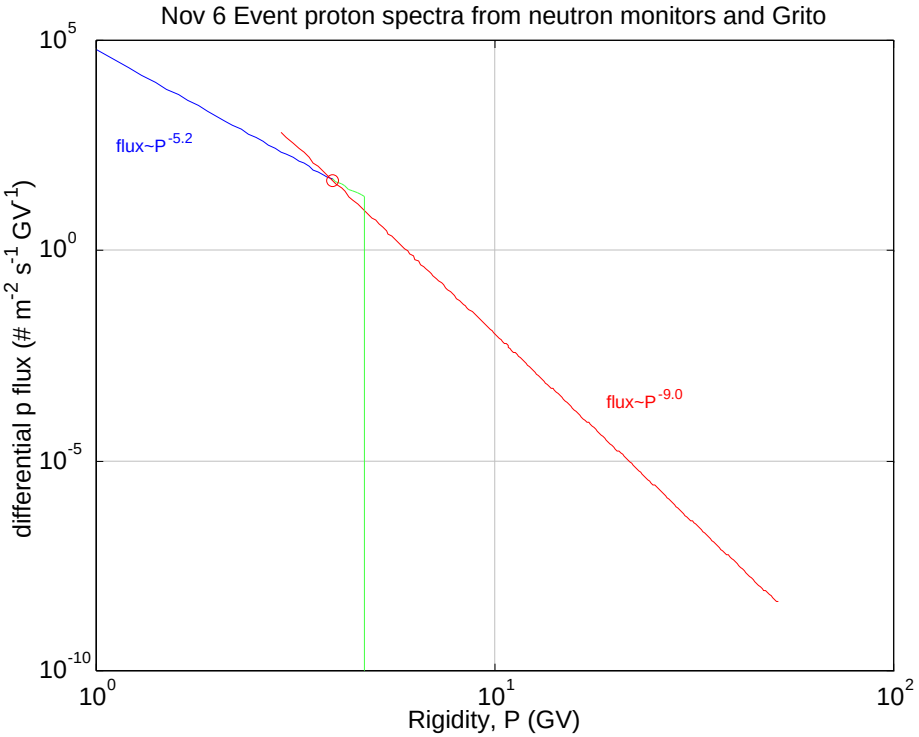

Fig. 8 - Calculated differential flux of isotropic protons from the 6 November 1997 SEP event. Below ~4 GV, the neutron monitor derived flux spectrum is shown. Above ~4 GV, two possible spectra that are consistent with the Milagrito high threshold scaler rate increase are shown. One of these spectra involves a hard cutoff of the spectrum from lower energies, while the other curve is a broken power law. The actual spectrum is probably a gradual rollover of the rigidity power law. The circle is placed at the point where the neutron monitor and the Milagrito derived spectra were required to overlap.

5. Event Timing

Prior to the detection of energetic particles at Earth, X-rays and gamma rays were detected by space-based instruments, and the CME-associated solar flare was categorized as X9. Yoshimori reported the detection of gamma rays up to 100 MeV, with an onset time of 11:52 UT for the 10-20 MeV emission (Yoshimori et al. 2000). See figure 9. Several lines were present in the spectrum derived from Yohkoh data, including the neutron capture line and C and O deexcitation lines. It is clear that proton acceleration

was occurring at the flare site for a short period of time following 11:52 UT. The gamma ray event, as measured with Yohkoh, was over within five minutes of onset.

The time profile measured by Milagrito is consistent with that of Climax, when allowances are made for the long-term, background meteorological fluctuations (Figures 4 and 5). The onset of the Milagrito scaler rate enhancement, which was at 12:07 UT +/- 6 min, was simultaneous within error with the Climax neutron monitor onset time, which was at approximately 12:06 UT. The times of maximum intensity and the duration are also similar. The rate in the Milagrito scalers, during the increase, reached its maximum value at 12:44 UT ± 6 min. The GOES satellite also observed an enhanced rate of

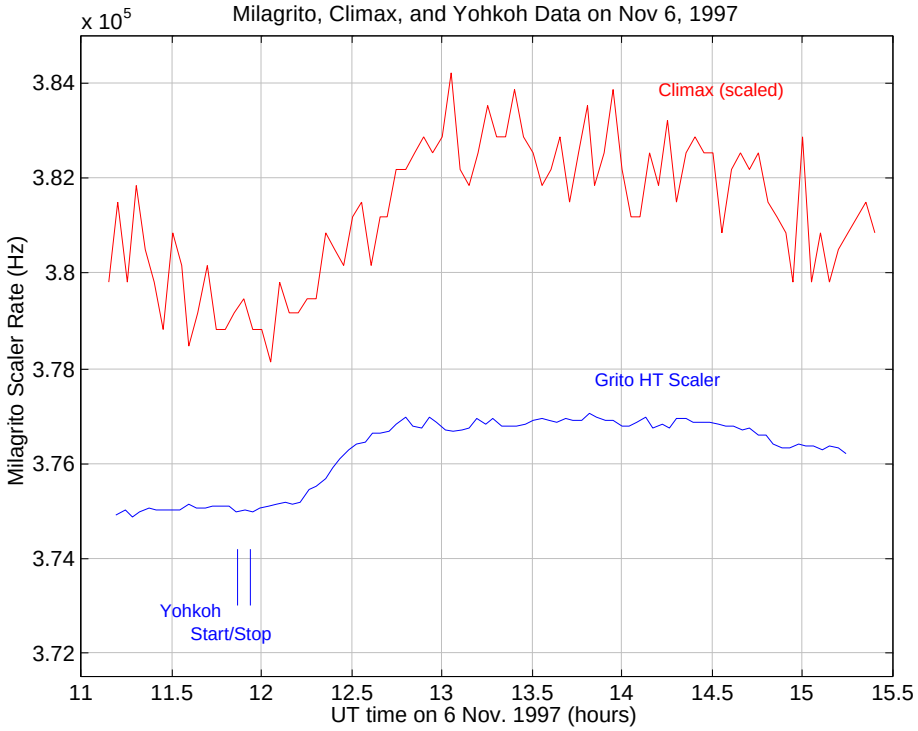

Fig. 9 – Onset of the Milagrito high threshold scaler rate increase and the Climax rate increase, with lines marking the beginning and end of the Yohkoh γ-ray line observations for comparison.

protons from this event, and the >100 MeV proton emission detected by the GOES satellite lasted more than two days. GOES also detected protons from an event that occurred on 4 November. While the flux of >100 MeV protons had returned to the pre-disturbance level by the time of the 6 Nov. event, the flux of >10 MeV protons was still elevated by a factor of ~10 over its background value measured prior to the 4 November event.

6. Discussion and Conclusions

When the short duration (~5 min) of the gamma ray line emission and the long duration (~hours to ~days, depending on energy) of the high energy proton acceleration are considered, it appears as though much of the proton acceleration does not occur in the flare itself. Although this analysis, by itself, does not rule out acceleration at the flare site with subsequent interplanetary diffusion, the simpler explanation is that of an extended CME shock front. Protons do appear to be accelerated at the flare site during the

impulsive phase, but the GeV protons, which come later, probably originate in the low corona. If a CME-driven shock was responsible for the GeV protons, then the height of the CME at the time at which protons reached these high energies can be estimated by looking at the difference in time between the gamma ray onset and the GLE onset, while accounting for the proton path length along the Parker spiral of the interplanetary magnetic field. A path length of 1.1±0.05 AU from the region around the flare site to Earth during the time of the 6 Nov 1997 event is expected, if any IMF disturbances are neglected (the error bars arise from the 1σ error bars in the input parameters, which means that kinks in the field lines and fluctuations of the magnetic field are neglected). The path length can also be affected by the pitch angle distribution of the particles. The path length calculation shown above does not account for the spiral path of a particle with a non-zero pitch angle. This tends to scale the path length by $(\cos \theta)^{-1}$. For instance, the path length would be double the Parker spiral value for a particle with a pitch angle of 60˚. Although the event exhibited some anisotropy in its early stages, it has already been stated that Lovell et al. (1998) found that the FWHM was ~60˚ at this time. However, the onset time of the event is determined by the earliest arriving particles, which were the ones with small pitch angles that were beamed along the IMF line. This leads to an estimate of ~10-20 minutes for the acceleration time of the >4 GV protons. After this amount of time, assuming a CME leading edge speed of ~2000 km/s, the leading edge of the CME was at ~2-4 solar radii.

This spatial scale is reasonable, and it is consistent with prior results on GeV ion acceleration heights found for the 24 May 1990 CME event studied by Lockwood et al. (1999) and the September 1989 event studied by Kahler (1992). In these studies, which made use of similar timing arguments, particle injection heights were calculated to be ~2 solar radii and ~2.5-4 solar radii, respectively. An acceleration time of ~10 minutes for ~1-10 GeV protons is consistent with the collisionless shock model of Lee & Ryan (1986), when injection energies of ~10 MeV are present. In this model, the ratio of injection energy to accelerated particle energy as a function of time was calculated. While this is a simple blast wave model, similar driven shock models could be applied (e.g. Lee 1997). Based on GOES data, there was an abundance of >10 MeV protons that continued to occupy interplanetary space due to the 4 November solar event. These ambient energetic protons could have provided the >10 MeV particle injection energies needed by the propagating CME-driven shock. While this does present a consistent interpretation, it is not definitive.

Between 10 and 60 MeV, the instruments on board the ACE satellite observed a proton spectrum of the form $E^{-2.1}$ (Cohen et al. 1999), while at higher energies, ground-based instruments observed much softer spectra. The Milagrito data, combined with neutron monitor data, leads to a proton spectrum with a rigidity power law spectral index of 9.0 ± 2.3, if a single power law is assumed above ~4 GV. A continuation of the $P^{-5.2}$ spectrum from Lovell et al. (1999) with a hard cutoff is also possible. These spectra are, by construction, continuous with the spectrum derived from the world wide neutron monitor network at 4 GV. In any case, the spectra derived from Milagrito and neutron monitor data provide evidence for a gradual rollover or a cutoff somewhere in Milagrito's sensitivity range above ~4 GV.

This steepened high energy spectrum is also consistent with a low corona origin based on the implied shock strength. For a differential rigidity power law spectral index of 9.0 ± 2.3 for relativistic protons to result from diffusive shock acceleration, one must have a shock compression ratio of ~1.2. For a fast CME, such as this, to drive a shock with this low compression ratio, the Alfven speed in the local medium must be relatively high. This shock compression ratio implies an Alfven speed on the high end of that expected in the solar corona. This implies that the acceleration occurred low in the

corona where the magnetic field and the Alfven speed were large. This is consistent with the timing arguments presented above for a low coronal origin. Once again, this presents a consistent picture, yet it is not definitive. It is also possible that the spectrum could be steepened by a transport effect after the diffusive shock acceleration occurs or that an unidentified alternative source could produce this steep spectrum.

The Milagro instrument, for which Milagrito was a prototype, is currently taking data (for more details on Milagro, see Atkins et al. 2001). With its increased number of PMTs, multiple layer design, increased effective area, and stable operation (relative to the engineering mode operation of Milagrito), Milagro may provide exciting results in the future. The number of PMTs in Milagro has increased to 723, relative to the 228 PMTs in Milagrito. These PMTs are arranged in two layers and they cover more physical area than was previously covered by Milagrito. Milagro's second layer of PMTs, submerged under 6.5 meters of water, can provide the ability to reconstruct the directions of single muons and small showers in the pond. In the future, this second layer could also be used to incorporate advanced triggering mechanisms. By using the pulse height information from this bottom layer of PMTs, one can identify penetrating muons. Timing information can then be used to reconstruct the incident direction of these muons. This technique will lower the energy threshold for reconstructable events. Proposed enhancements to the data acquisition system, which would allow Milagro to record this higher rate data and reconstruct hadronic events down to primary energies of ~3 GeV, may further increase Milagro's capabilities, particularly its ability to study solar energetic particles (Ryan et al. 2000).

Acknowledgements

We acknowledge the contributions of many people who helped construct and operate Milagrito. In particular, we thank R.S.Delay, M.Schneider, and T.N.Thompson, who were indispensable during the construction, maintenance, and operation of the detector. We also thank E. Cliver, J.Gosling, M. Lee, and J.Lockwood for their helpful comments and discussions.

This work was supported in part by the National Science Foundation, the US Department of Energy Office of High Energy Physics, the US Department of Energy Office of Nuclear Physics, Los Alamos National Laboratory, the University of California, the Institute of Geophysics and Planetary Physics, the Research Corporation, the California Space Institute, and the University of New Hampshire Space Science Center.

References

Atkins, R., et al. 2000, *Nuclear Instruments & Methods in Physics Research A*, **449**, 478.
CERN Application Software Group 1994, CERN W, 5013, Version 3.21.
Chiba, N., et al. 1992, *Astroparticle Physics*, **1**, 27.
Cohen, C.M.S., et al. 1999, *Geophys. Res. Lett.*, **26**, 149.
Debrunner, H. 1994, in *AIP Conf. Proc. # 294: High Energy Solar Phenomena*, Ryan, J.M. & Vestrand, W.T. eds. (New York: AIP press).
Duldig, M.L. and Humble, J.E. 1999, in *Proc. XXV! Int. Cosmic Ray Conf*, **6**, 403.
Falcone, A.D., et al. 1999, *Astroparticle Physics*, **11**, 283.
Fowler, G.N., Wolfendale, A.W., and Flugge, S., eds. 1961, *Cosmic Rays I.*
GOES 2001, http://www.sec.noaa.gov/
Gosling, J.T. 1993, *Journ. of Geophys. Research*, **98** (A11), 18937.
Hayakawa, S. 1969, *Cosmic Ray Physics* (New York: John Wiley and Sons).
Heck, D. 1999, *private communication*

Heck, D., et al. 1998, *Corsika: A Monte Carlo Code to Simulate Extensive Air Showers*, Forschungszentrum Karlsruhe Report FZKA 6019.
Kahler, S.W. 1994, *Astrophys. J.*, **428**, 837.
Kahler, S.W. 1992, *Annu. Rev. Astron & Astrophys.*, **30**, 113.
Lee, M.A. 1997, in *American Geophys. Union Monograph 99: Coronal Mass Ejections*, eds. Crooker, N., Joselyn, J., & Feynman, J., 227.
Lee, M.A., and Ryan, J.M. 1986, *Astrophys. J.*, **303**, 829.
Lockwood, J.A., Debrunner, H., Ryan, J.M. 1999, *Astroparticle Physics*, **12**, 97.
Lovell, J.L., et al. 1999, *Adv. Space Res.*
Lovell, J.L., Duldig, M.L., Humble, J.E. 1998, *Journ. of Geophys. Research*, **103**, 23733.
Maia, D., et al. 1999, *Journ. Geophys. Res*, **104**, 12507.
Mason, G.M., et al. 1999, *Geophys. Res. Lett.*, **26**, 141.
McCullough, J.F., et al. 1999, in *Proc. XXVI Int. Cosmic Ray Conf.*, **2**, 369.
Meyer, P., Parker, E.N., Simpson, J.A. 1956, *Physical Review*, **104**, 768.
Mobius, E, et al. 1999, *Geophys. Res. Lett.*, **26**, 145.
Parker, E.N. 1957, *Physical Review*, **107**, 830.
Reames, D.V. 1999, *Space Science Reviews*, **90**, 413.
Ryan, J.M. et al. 2000, in *AIP Conf. Proc. 528: Acceleration and Transport of Energetic Particles Observed in the Heliosphere*, eds. Mewaldt, R.A., et al., 197.
Ryan, J.M. et al. 1999, in *Proc. of the XXVI International Cosmic Ray Conf.*, **6**, 378.
Sato, J., et al. 2000, *Adv. Space Res.*, **26**(3), 501.
Simpson, J.A. 1957, Ann. I.G.Y., part 7, Pergamon Press, London.
Smart, D.F. & Shea, M.A. 1998, in *Proc. Spring American Geophys. Union Mtg.*
St. Cyr, C. 2001, *private communication*.
Yoshimori, M., et al. 2000, in *AIP Conf. Proc. 528: Acceleration and Transport of Energetic Particles Observed in the Heliosphere*, eds. Mewaldt, R.A., et al., 189.